AJRCMB Articles in Press. Published on 18-December-2018 as 10.1165/rcmb.2018-0118OC

Lung Adenocarcinoma Syndecan-2 Potentiates Cell Invasiveness

Konstantin Tsoyi[1#], Juan C Osorio[1,2#], Sarah G Chu[1], Isis E Fernandez[3], Sergio Poli[1], Lynette Sholl[4], Ye Cui[1], Carmen S Tellez[5], Jill M Siegfried[6], Steven A Belinsky[5], Mark A. Perrella[1], Souheil El-Chemaly[1], Ivan O. Rosas[1,7]

[1]Division of Pulmonary and Critical Care Medicine, Brigham and Women's Hospital, Harvard Medical School, Boston, MA, [2]Department of Medicine, New York Presbyterian Hospital, Weill Cornell Medical College, New York, NY, [3]Comprehensive Pneumology Centre, Hospital of the Ludwig-Maximilians, University of Munich, Munich, [4]Department of Pathology, Brigham and Women's Hospital, Harvard Medical School, Boston, MA, [5]Lung Cancer Program, Lovelace Respiratory Research Institute, Albuquerque, NM, [6]University of Minnesota, Department of Pharmacology, Minneapolis, Minnesota, United States, [7]Pulmonary Fibrosis Group, Lovelace Respiratory Research Institute, Albuquerque NM

[#] Authors contributed equally to this work

Running title: Syndecan-2 is elevated in lung adenocarcinoma

Corresponding Author:

Ivan O. Rosas, M.D., Division of Pulmonary and Critical Care Medicine, Brigham and Women's Hospital, 75 Francis Street, Boston, MA 02115.

E-mail: irosas@rics.bwh.harvard.edu

Author Contributions: K.T., J.C.O., S.G.C., and I.O.R. designed the study, K.T., J.C.O., I.E.F., S.P., L.S., Y.C., C.S.T., S.A.B., performed the experiments, contributed materials and analysed data, J.M.S., M.A.P., S.E.C., contributed intellectual input, K.T., S.G.C., J.C.O., and I.O.R. wrote the manuscript.

Funding Information: Dr. Ivan O. Rosas was supported by NHLBI P01 HL114501. Dr. Konstantin Tsoyi was supported by NHLBI T32 5T32HL007633-32. Dr. Steven A Belinsky was supported by NCI Cancer Center Support Grant P30CA11800.

Key Words: Syndecan-2, syntenin-1, lung adenocarcinoma, metastasis

Abstract

Rationale: Altered expression of syndecan-2, a heparan sulfate proteoglycan, has been associated with diverse types of human cancers. However, the mechanisms by which syndecan-2 may contribute to the pathobiology of lung adenocarcinoma have not been previously explored.

Methods: Syndecan-2 levels were measured in human lung adenocarcinoma samples and Lung Cancer Tissue Microarrays using immunohistochemistry and real time-PCR. To understand the role of syndecan-2 *in vitro*, SDC2 was silenced or overexpressed in A549 lung adenocarcinoma cells. The invasive capacity of cells was assessed using Matrigel invasion assays and measuring matrix metalloproteinase 9 (mmp9) expression. Finally, we assessed tumor growth and metastasis of SDC2-deficient A549 cells in a xenograft tumor model.

Results: Syndecan-2 expression was upregulated in malignant epithelial cells and macrophages obtained from human lung adenocarcinomas. Silencing of SDC2 decreased mmp9 expression and attenuated the invasive capacity of A549 lung adenocarcinoma cells. The inhibitory effect of SDC2 silencing on mmp9 expression and cell invasion was reversed by overexpression of mmp9 and syntenin-1. SDC2 silencing attenuated NF-κB p65 subunit nuclear translocation and its binding to the MMP9 promoter, which were restored by overexpression of syntenin-1. SDC2 silencing *in vivo* reduced tumor mass volume and metastasis.

Conclusions: These findings suggest that syndecan-2 plays an important role in the invasive properties of lung adenocarcinoma cells and that its effects are mediated by syntenin-1. Thus, inhibiting syndecan-2 expression or activity could serve as a potential therapeutic target to treat lung adenocarcinoma.

AJRCMB Articles in Press. Published on 18-December-2018 as 10.1165/rcmb.2018-0118OC

Introduction

Lung cancer is the leading cause of cancer mortality in both men and women in the United States (1) and worldwide. An estimated 234,030 new lung cancer cases and 154,050 lung cancer deaths are projected to occur in the United States in 2018 (2). Despite advances in surgical techniques and novel therapeutic interventions such as targeted therapy and immune checkpoint blockade, 5-year survival remains elevated at 17% (3) and the molecular mechanisms that drive lung tumorigenesis continue to be poorly understood.

Syndecans, a family of type 1 transmembrane heparan sulfate proteoglycans consisting of four members (syndecans 1-4), have been implicated in the regulation of several types of cancer (4-7). Syndecans play a role in the control of cell adhesion, survival, proliferation, migration and differentiation. These pleiotropic activities are mediated by interactions of the syndecan ectodomain and its glycosaminoglycan chains with extracellular matrix and cell surface proteins, proteases, cytokines and their receptors. Some of these interactions are transduced through a single transmembrane domain to a short, highly conserved, cytoplasmic tail that tethers syndecans to intracellular structural proteins and signaling pathways (8).

Syndecan-2 is mainly expressed in cells of mesenchymal origin but has been shown to exert effects on several cell types. We have previously demonstrated the role of syndecan-2 in epithelial cells and fibroblast in the setting of idiopathic pulmonary fibrosis (9) and radiation-induced pulmonary fibrosis (10), respectively. Ectopic or overexpression of this proteoglycan has also been associated with the tumorigenic properties and poor prognosis of various malignancies, including colon (11, 12) and prostate adenocarcinomas (13, 14), melanoma (15, 16) and fibrosarcoma (17). It has been shown to also potentiate angiogenesis, as downregulation of syndecan-2 expression at the surface of microvascular endothelial cells reduces angiogenic sprouting (18-20). Conversely, elevated levels of syndecan-2 have been associated with decreased migration of human osteosarcoma cells and increased sensitivity to chemotherapy-induced apoptosis (21).

The role of syndecan-2 in lung adenocarcinoma, the most common form of lung cancer, has not been well characterized. Here we demonstrate that syndecan-2 is highly expressed in human lung adenocarcinomas and contributes to cancer cell invasion, matrix metalloproteinase-9 (mmp9) expression, tumor growth and metastasis. We further show that this is mediated by syntenin-1 and NF-κB activation.

Materials and Methods

Human Samples

All human samples were obtained under Institutional Review Board (IRB)-approved protocols at the University of New Mexico (Albuquerque, NM), the University of Pittsburgh Cancer Institute (Pittsburgh, PA) or Brigham and Women's Hospital (Boston, MA). Control human lung samples without malignancy were obtained from donor lungs deemed unsuitable for transplantation.

Antibodies

Anti-mmp9 and anti-NF-κB (p65) antibodies were purchased from Cell Signaling Technology (Danvers, MA), anti-syndecan-2 from Thermo Scientific (Waltham, MA) and anti-syntenin-1 from Santa Cruz Biotechnology (Santa Cruz, CA). All other antibodies and associated reagents were purchased from Sigma-Aldrich (St. Louis, MO).

Immunohistochemistry

Immunostaining of lung tissue from lung biopsies and tissue arrays was performed as previously described (22). Lung Cancer Tissue MicroArrays (LTMA) were obtained from Pantomics (Cat. #: LUC481, LUC961 and LUC962; San Francisco, CA). Briefly, sections were incubated in citric acid buffer (pH 6.0) at 95 ºC for 30 min for the purpose of antigen retrieval. Sections were then incubated in 1% BSA for blocking non-specific binding of the antibody. A polyclonal antibody for syndecan-2 was prepared in dilution of 1:500 and applied to the sections overnight at 4 ºC. Sections were stained using the HRP-DAB System (Cell &

AJRCMB Articles in Press. Published on 18-December-2018 as 10.1165/rcmb.2018-0118OC

Tissue Staining Kit) according to the manufacturer's instructions, and then counterstained with hematoxylin and eosin. The amount of staining was scored from 1 to 4 (lowest to highest, respectively). The score was determined by staining intensity in conjunction with the percentage of cells staining positively, counting 10 random fields at 200 X magnification in tissue sections. Slides were independently scored by three investigators using an Olympus BX40 microscope (Olympus, Melville, NY).

Cell Culture

A549 cells were obtained from American Type Tissue Culture Collection (ATCC, Manassas, VA) and cultured according to the manufacturer's instructions in DMEM supplemented with 10% fetal bovine serum (FBS), penicillin (100 units/mL), and streptomycin (10 μg/mL) (Invitrogen, Carlsbad, CA).

Statistical Analysis

Data are expressed as mean ± SEM. Comparisons of mortality were made by analyzing Kaplan-Meier survival curves and log-rank tests to assess for differences in survival. For comparisons between two groups, we used Student's unpaired t test and statistical significance defined as $p<0.05$. One-way analysis of variance, followed by Newman-Keuls or Tukey's post-test analysis, was used for analysis of more than two groups. The numbers of samples per group (n), or the numbers of experiments, are specified in the figure legends.

For additional details regarding materials and methods, please see online supplement.

Results

Syndecan-2 Expression is Upregulated in Human Lung Adenocarcinoma

Immunostaining of lung tissue sections from patients with lung adenocarcinoma revealed that syndecan-2 was highly expressed in malignant epithelial cells in the tumor core, while in

the tumor-free margins it was mainly expressed in macrophages (Figure 1A). Syndecan-2 mRNA levels were also significantly elevated in the tumor core compared to the tumor-free margins (Figure 1B). We also assessed syndecan-2 expression using a Lung Cancer Tissue MicroArray (LTMA) and observed a significant increase in syndecan-2 staining in human lung adenocarcinoma tissue compared to control lung tissue (Figure 1C). Syndecan-2 expression was also increased in other types of lung carcinomas (Figure E1). To determine whether our findings were specific to syndecan-2, we measured syndecan-1 and syndecan-2 mRNA levels in lung adenocarcinoma tissue and control lungs without cancer (n=9 per group). Syndecan-2 mRNA was increased 5 to 35-fold in lung adenocarcinomas compared to controls (Figure 1D). In contrast, there was no significant difference in syndecan-1 mRNA expression.

Taken together, these findings demonstrate that syndecan-2 expression is upregulated in lungs from patients with lung adenocarcinoma and that malignant epithelial cells are the main source of this heparan sulfate proteoglycan.

Syndecan-2 Increases Mmp9 Expression and Activity and is Associated with Enhanced Invasive Activity of A549 Lung Adenocarcinoma Cells

We next sought to establish the role of syndecan-2 in the malignant properties of lung adenocarcinoma. Matrix metalloproteinase protein-9 (mmp9) has been strongly correlated with tumor malignant potential and poor patient survival, especially in lung cancer (23, 24). Mmp9 is regulated by NF-κB signalling, which has been associated with poor prognosis in non-small cell lung cancers (25). Mmp9 inhibition has been reported to attenuate cancer cell invasion and metastasis (26, 27). We found an increased expression of syndecan-2, NF-κB (p65) and mmp9 in lung adenocarcinoma tissue (Figure E2). While syndecan-2 has previously been shown to act as a docking protein for mmp7 in colon cancer (11), it is unknown whether it modulates mmp9 activity. Accordingly, we investigated the potential interaction between syndecan-2 and mmp9 in a lung adenocarcinoma cell line. Silencing of

AJRCMB Articles in Press. Published on 18-December-2018 as 10.1165/rcmb.2018-0118OC

SDC2 in A549 cells reduced their invasive capacity as determined by a Matrigel invasion assay (Figure 2A), significantly decreased mmp9 gene and protein expression, and attenuated its enzymatic activity (Figures 2B and 2C). SDC2 silencing had a similar effect on cell invasiveness and mmp9 expression in NCI-H23 cells, another lung adenocarcinoma cell line (Figure E3B).

We hypothesized that syndecan-2 overexpression would conversely enhance mmp9 expression and cell invasion. A549 cells were lentivirally transfected with human SDC2 plasmids tagged with GFP (Figure 3A). Overexpression of syndecan-2 increased mmp9 expression and Matrigel invasion (Figures 3B and 3C). Cell invasion was significantly increased compared to controls at 8 hours but not at 24 hours, possibly due to the high levels of endogenous syndecan-2 expressed in A549 cells which may have diminished the early effects of syndecan-2 overexpression over time.

Mmp9 Regulates Cell Invasiveness and Overexpression Reverses Syndecan-2-Mediated Cell Invasion

To confirm that mmp9 is an important contributor in lung adenocarcinoma invasiveness, we silenced MMP9 using shRNA lentiviral particles and found that this significantly reduced cell invasion in A549 cells (Figures 4A and 4B). Conversely, overexpression of mmp9 in A549 cells by pCMV6-MMP9 transfection enhanced cell invasion and completely reversed shSDC2-mediated inhibition of cell invasion (Figure 4C). These data suggest that mmp9 plays a critical role in A549 cell invasiveness and that syndecan-2 mediates cell invasion via regulation of mmp9.

Syntenin-1 Facilitates Syndecan-2-Mediated MMP9 Expression and Cell Invasion

Syntenin-1 is an adaptor molecule involved in diverse cellular processes, including protein trafficking, cell adhesion and tumorigenesis. It has been previously shown that syntenin-1 can be activated by binding to the PDZ region of the cytosolic tail of syndecan-2, which in

turn activates a variety of signaling molecules such as MAPKs and NF-κB (28-30). We confirmed that syntenin-1 binds to syndecan-2 in A549 cells and that this binding is abolished by silencing of SDC2 (Figure 5A). We then assessed whether syntenin-1 mediates the invasive effects of syndecan-2 in A549 cells. Overexpression of syntenin-1 almost completely restored mmp9 expression and the invasive capacity of cells in which SDC2 was silenced, suggesting that syntenin-1 is necessary for syndecan-2-mediated invasion (Figure 5B-5D).

Syndecan-2 Regulates NF-κB Activation through Syntenin-1

It has previously been suggested that syntenin-1 may be involved in the activation of NF-κB (31, 32), a master regulator of cancer cell metastasis and gene expression. In light of our findings showing that NF-κB expression is elevated in human lung adenocarcinomas (Figure E2) and that syndecan-2 regulates A549 cell invasion via syntenin-1, we asked whether syndecan-2 also modulates NF-κB activation. As shown in Figure 6A, nuclear translocation of the p65 subunit of NF-κB was significantly lower in shSDC2-transfected A549 cells than in scramble-transfected cells. Syntenin-1 overexpression restored p65 nuclear translocation. Furthermore, silencing of SDC2 significantly attenuated p65 binding to the MMP9 promoter, but not in cells overexpressing syntenin-1 (Figure 6B). Knockdown of p65 significantly reduced mmp9 expression and cell invasion (Figures 6C and 6D). These data strongly suggest that syndecan-2 regulates MMP9 expression via syntenin-1 and NF-κB activation to facilitate cell invasion.

Syndecan-2 Silencing Attenuates Growth and Metastasis of A549 Cells in SCID Mice

To evaluate the effect of syndecan-2 on tumor progression *in vivo*, scramble or shSDC2-transfected A549 adenocarcinoma cells were subcutaneously injected into severe combined immunodeficient (SCID) mice. Consistent with our *in vitro* findings, silencing of SDC2 with targeted shRNA significantly attenuated tumor growth (Figures 7A and 7B) and micro-

AJRCMB Articles in Press. Published on 18-December-2018 as 10.1165/rcmb.2018-0118OC

metastasis to the lungs (Figure 7C) in SCID mice, further highlighting the role of syndecan-2 in potentiating adenocarcinoma cell invasion.

Discussion

Tumor metastasis is the primary cause of morbidity and mortality in patients with cancer (33). It is a complex process in which diverse interactions between cancer cells and their microenvironment enable malignant cells to invade the tissue surrounding the primary neoplasm, enter the circulation via the bloodstream or lymphatics, and populate distant locations (33). Proteolysis of tissue barriers is an essential component of the invasive process and has been linked to the production of degradative enzymes by cancer cells, the most intensively studied being matrix metalloproteinases (34). MMPs are a group of proteins with a variety of cellular and extracellular functions, including extracellular matrix degradation (24). To date, 23 different MMPs have been identified in humans. Mmp9, also known as gelatinase B, has been shown to play a prominent role in tumor malignant potential and lung-specific metastasis (23, 35). Higher levels of mmp9 are correlated with poor patient prognosis in non-small cell lung cancer (36), and mmp9 inhibition has been reported to attenuate cancer cell invasion and metastasis (26, 27).

Syndecans interact with multiple proteins in the extracellular environment, including cytokines and their receptors, through their highly divergent ectodomains (37). High levels of syndecan-2 have been detected in diverse cancers and are associated with cancer cell migration, invasion and proliferation. On the other hand, shed syndecan-2 has been shown to inhibit angiogenesis, a critical feature of metastasis, by activating membrane-bound protein tyrosine phosphotase eta (PTPRj) (38). The role of syndecan-2 in lung adenocarcinoma has not been extensively studied (39).

In this study, we report for the first time that syndecan-2 is significantly elevated in malignant lung epithelial cells of patients with lung adenocarcinoma as well as other lung cancer types. Using loss- and gain-of-function experiments, we demonstrate that syndecan-2 plays an important role in lung adenocarcinoma cell invasion and mmp9 expression and

activity. Furthermore, silencing of SDC2 in A549 cells significantly reduced tumor growth and cancer cell metastasis in a xenograft tumor model. Interestingly, syndecan-2 was also detected in the tumor stroma of lung adenocarcinoma (Figure 1A). Elevated expression of syndecan-1 has been observed in tumor stromal cells and is associated with poor prognosis (40) and expression of syndecan-1 in fibroblasts enhances tumor growth and angiogenesis *in vivo* and *in vitro* (41). Future studies should be dedicated to evaluate the role of syndecan-2 in cancer-associated stromal cells, as well as correlate syndecan-2 expression to lung adenocarcinoma histological subtypes, lymphovascular invasion, metastases and clinical outcomes.

In contrast to our findings, Munesue *et al.* (42) demonstrated that overexpression of syndecan-2 is associated with decreased metastatic potential in cells cloned from Lewis lung carcinoma 3LL, by suppressing the activity of mmp2. However, the 3LL clones used in these experiments only expressed mmp2 in the extracellular matrix, suggesting that the biological effects of syndecan-2 are highly dependent on their interactions with specific heparin-binding extracellular ligands, and that the balance between mmp2 and mmp9 expression may be critical in determining the role of syndecan-2 in the tumor microenvironment.

The cytoplasmic domain of syndecan-2 has been shown to interact with different adapter proteins. These include PDZ proteins such as syntenin. Syntenin, a PDZ domain-containing adapter protein, originally identified as a syndecan-binding protein, is known to be involved in the organization of protein complexes in the plasma membrane. Syntenin plays a well-described role in cell migration and invasion in different cancer cell types (30-32, 43, 44). In this study, we demonstrate that syntenin-1 interacts with syndecan-2 and that overexpression of syntenin-1 restores the invasive phenotype in SDC2-silenced lung adenocarcinoma cells. It has recently been shown that syntenin-1 tightly regulates the epithelial-mesenchymal transition (EMT) in TGF-β-induced lung adenocarcinoma epithelial cells (45, 46). Further investigation is needed to understand the role of syndecan-2 in EMT.

Previous reports suggest that the pro-metastatic role of syntenin is mediated by NF-κB activation (44, 45). NF-κB is well established as a master regulator of multiple genes

AJRCMB Articles in Press. Published on 18-December-2018 as 10.1165/rcmb.2018-0118OC

involved in cancer cell metastasis, including MMPs (47). Our findings clearly demonstrate that syndecan-2 regulates the NF-κB p65 subunit cytosol to nuclear translocation and its binding to the MMP9 promoter via syntenin-1. This further supports the role of syndecan-2 in enhancing the invasive capacity of lung cancer cells.

Taken together, these findings demonstrate the important role of syndecan-2 in mediating lung adenocarcinoma cell invasion, and highlight its potential as a target for therapeutic interventions to treat lung adenocarcinomas.

Acknowledgements:

We thank Yuanyuan Shi and Xiaomeng Tang for their technical support.

Disclosures:

No conflicts of interest reported.

References:

1. Torre LA, Siegel RL, Ward EM, Jemal A. Global cancer incidence and mortality rates and trends--an update. *Cancer Epidemiol Biomarkers Prev* 2016;25(1):16-27.
2. Siegel RL, Miller KD, Jemal A. Cancer statistics, 2018. *CA Cancer J Clin* 2018;68(1):7-30.
3. Siegel R, DeSantis C, Virgo K, Stein K, Mariotto A, Smith T, Cooper D, Gansler T, Lerro C, Fedewa S, et al. Cancer treatment and survivorship statistics, 2012. *CA: a cancer journal for clinicians* 2012;62(4):220-241.
4. Iozzo RV, Sanderson RD. Proteoglycans in cancer biology, tumour microenvironment and angiogenesis. *J Cell Mol Med* 2011;15(5):1013-1031.
5. Labropoulou VT, Skandalis SS, Ravazoula P, Perimenis P, Karamanos NK, Kalofonos HP, Theocharis AD. Expression of syndecan-4 and correlation with metastatic potential in testicular germ cell tumours. *Biomed Res Int* 2013;2013:214864.
6. Suhovskih AV, Mostovich LA, Kunin IS, Boboev MM, Nepomnyashchikh GI, Aidagulova SV, Grigorieva EV. Proteoglycan expression in normal human prostate tissue and prostate cancer. *ISRN Oncol* 2013;2013:680136.
7. Nguyen TL, Grizzle WE, Zhang K, Hameed O, Siegal GP, Wei S. Syndecan-1 overexpression is associated with nonluminal subtypes and poor prognosis in advanced breast cancer. *Am J Clin Pathol* 2013;140(4):468-474.
8. Choi Y, Chung H, Jung H, Couchman JR, Oh ES. Syndecans as cell surface receptors: Unique structure equates with functional diversity. *Matrix Biol* 2011;30(2):93-99.
9. Shi Y, Gochuico BR, Yu G, Tang X, Osorio JC, Fernandez IE, Risquez CF, Patel AS, Wathelet MG, Goodwin AJ, et al. Syndecan-2 exerts antifibrotic effects by promoting caveolin-1-mediated transforming growth factor-beta receptor i internalization and inhibiting transforming growth factor-beta1 signaling. *Am J Respir Crit Care Med*;188(7):831-841.

10. Tsoyi K, Chu SG, Patino-Jaramillo NG, Wilder J, Villalba J, Doyle-Eisele M, McDonald J, Liu X, El-Chemaly S, Perrella MA, et al. Syndecan-2 attenuates radiation-induced pulmonary fibrosis and inhibits fibroblast activation by regulating pi3k/akt/rock pathway via cd148. *Am J Respir Cell Mol Biol* 2018;58(2):208-215.
11. Park H, Kim Y, Lim Y, Han I, Oh ES. Syndecan-2 mediates adhesion and proliferation of colon carcinoma cells. *The Journal of biological chemistry* 2002;277(33):29730-29736.
12. Choi S, Kim JY, Park JH, Lee ST, Han IO, Oh ES. The matrix metalloproteinase-7 regulates the extracellular shedding of syndecan-2 from colon cancer cells. *Biochemical and biophysical research communications* 2012;417(4):1260-1264.
13. Contreras HR, Ledezma RA, Vergara J, Cifuentes F, Barra C, Cabello P, Gallegos I, Morales B, Huidobro C, Castellon EA. The expression of syndecan-1 and -2 is associated with gleason score and epithelial-mesenchymal transition markers, e-cadherin and beta-catenin, in prostate cancer. *Urologic oncology* 2010;28(5):534-540.
14. Popovic A, Demirovic A, Spajic B, Stimac G, Kruslin B, Tomas D. Expression and prognostic role of syndecan-2 in prostate cancer. *Prostate cancer and prostatic diseases* 2010;13(1):78-82.
15. Lee JH, Park H, Chung H, Choi S, Kim Y, Yoo H, Kim TY, Hann HJ, Seong I, Kim J, et al. Syndecan-2 regulates the migratory potential of melanoma cells. *The Journal of biological chemistry* 2009;284(40):27167-27175.
16. Baljinnyam E, Iwatsubo K, Kurotani R, Wang X, Ulucan C, Iwatsubo M, Lagunoff D, Ishikawa Y. Epac increases melanoma cell migration by a heparan sulfate-related mechanism. *American journal of physiology Cell physiology* 2009;297(4):C802-813.
17. Park H, Han I, Kwon HJ, Oh ES. Focal adhesion kinase regulates syndecan-2-mediated tumorigenic activity of ht1080 fibrosarcoma cells. *Cancer Res* 2005;65(21):9899-9905.
18. Fears CY, Gladson CL, Woods A. Syndecan-2 is expressed in the microvasculature of gliomas and regulates angiogenic processes in microvascular endothelial cells. *The Journal of biological chemistry* 2006;281(21):14533-14536.
19. Chen E, Hermanson S, Ekker SC. Syndecan-2 is essential for angiogenic sprouting during zebrafish development. *Blood* 2004;103(5):1710-1719.
20. Noguer O, Villena J, Lorita J, Vilaro S, Reina M. Syndecan-2 downregulation impairs angiogenesis in human microvascular endothelial cells. *Exp Cell Res* 2009;315(5):795-808.
21. Orosco A, Fromigue O, Bazille C, Entz-Werle N, Levillain P, Marie PJ, Modrowski D. Syndecan-2 affects the basal and chemotherapy-induced apoptosis in osteosarcoma. *Cancer Res* 2007;67(8):3708-3715.
22. Valencia JC, Pacheco-Rodriguez G, Carmona AK, Xavier J, Bruneval P, Riemenschneider WK, Ikeda Y, Yu ZX, Ferrans VJ, Moss J. Tissue-specific renin-angiotensin system in pulmonary lymphangioleiomyomatosis. *Am J Respir Cell Mol Biol* 2006;35(1):40-47.
23. van Kempen LC, Coussens LM. Mmp9 potentiates pulmonary metastasis formation. *Cancer cell* 2002;2(4):251-252.
24. Visse R, Nagase H. Matrix metalloproteinases and tissue inhibitors of metalloproteinases: Structure, function, and biochemistry. *Circulation research* 2003;92(8):827-839.
25. Gu L, Wang Z, Zuo J, Li H, Zha L. Prognostic significance of nf-kappab expression in non-small cell lung cancer: A meta-analysis. *PloS one* 2018;13(5):e0198223.
26. Kim YM, Tsoyi K, Jang HJ, Park EJ, Park SW, Kim HJ, Hwa JS, Chang KC. Ckd712, a synthetic isoquinoline alkaloid, enhances the anti-cancer effects of paclitaxel in mda-mb-231 cells through regulation of pten. *Life sciences* 2014;112(1-2):49-58.
27. Li G, He Y, Yao J, Huang C, Song X, Deng Y, Xie S, Ren J, Jin M, Liu H. Angelicin inhibits human lung carcinoma a549 cell growth and migration through regulating jnk and erk pathways. *Oncology reports* 2016;36(6):3504-3512.
28. Zimmermann P, Tomatis D, Rosas M, Grootjans J, Leenaerts I, Degeest G, Reekmans G, Coomans C, David G. Characterization of syntenin, a syndecan-binding pdz protein, as a component of cell adhesion sites and microfilaments. *Molecular biology of the cell* 2001;12(2):339-350.

AJRCMB Articles in Press. Published on 18-December-2018 as 10.1165/rcmb.2018-0118OC

29. Grootjans JJ, Zimmermann P, Reekmans G, Smets A, Degeest G, Durr J, David G. Syntenin, a pdz protein that binds syndecan cytoplasmic domains. *Proceedings of the National Academy of Sciences of the United States of America* 1997;94(25):13683-13688.
30. Kegelman TP, Das SK, Hu B, Bacolod MD, Fuller CE, Menezes ME, Emdad L, Dasgupta S, Baldwin AS, Bruce JN, et al. Mda-9/syntenin is a key regulator of glioma pathogenesis. *Neuro-oncology* 2014;16(1):50-61.
31. Boukerche H, Aissaoui H, Prevost C, Hirbec H, Das SK, Su ZZ, Sarkar D, Fisher PB. Src kinase activation is mandatory for mda-9/syntenin-mediated activation of nuclear factor-kappab. *Oncogene* 2010;29(21):3054-3066.
32. Boukerche H, Su ZZ, Emdad L, Sarkar D, Fisher PB. Mda-9/syntenin regulates the metastatic phenotype in human melanoma cells by activating nuclear factor-kappab. *Cancer Res* 2007;67(4):1812-1822.
33. Steeg PS. Tumor metastasis: Mechanistic insights and clinical challenges. *Nature medicine* 2006;12(8):895-904.
34. Herszenyi L, Hritz I, Lakatos G, Varga MZ, Tulassay Z. The behavior of matrix metalloproteinases and their inhibitors in colorectal cancer. *International journal of molecular sciences* 2012;13(10):13240-13263.
35. Hiratsuka S, Nakamura K, Iwai S, Murakami M, Itoh T, Kijima H, Shipley JM, Senior RM, Shibuya M. Mmp9 induction by vascular endothelial growth factor receptor-1 is involved in lung-specific metastasis. *Cancer cell* 2002;2(4):289-300.
36. Gong L, Wu D, Zou J, Chen J, Chen L, Chen Y, Ni C, Yuan H. Prognostic impact of serum and tissue mmp-9 in non-small cell lung cancer: A systematic review and meta-analysis. *Oncotarget* 2016;7(14):18458-18468.
37. Leonova EI, Galzitskaya OV. Cell communication using intrinsically disordered proteins: What can syndecans say? *J Biomol Struct Dyn*:1-14.
38. De Rossi G, Evans AR, Kay E, Woodfin A, McKay TR, Nourshargh S, Whiteford JR. Shed syndecan-2 inhibits angiogenesis. *Journal of cell science* 2014;127(Pt 21):4788-4799.
39. Munesue S, Kusano Y, Oguri K, Itano N, Yoshitomi Y, Nakanishi H, Yamashina I, Okayama M. The role of syndecan-2 in regulation of actin-cytoskeletal organization of lewis lung carcinoma-derived metastatic clones. *The Biochemical journal* 2002;363(Pt 2):201-209.
40. Szarvas T, Reis H, Kramer G, Shariat SF, Vom Dorp F, Tschirdewahn S, Schmid KW, Kovalszky I, Rubben H. Enhanced stromal syndecan-1 expression is an independent risk factor for poor survival in bladder cancer. *Human pathology* 2014;45(4):674-682.
41. Maeda T, Desouky J, Friedl A. Syndecan-1 expression by stromal fibroblasts promotes breast carcinoma growth in vivo and stimulates tumor angiogenesis. *Oncogene* 2006;25(9):1408-1412.
42. Munesue S, Yoshitomi Y, Kusano Y, Koyama Y, Nishiyama A, Nakanishi H, Miyazaki K, Ishimaru T, Miyaura S, Okayama M, et al. A novel function of syndecan-2, suppression of matrix metalloproteinase-2 activation, which causes suppression of metastasis. *The Journal of biological chemistry* 2007;282(38):28164-28174.
43. Das SK, Guo C, Pradhan AK, Bhoopathi P, Talukdar S, Shen XN, Emdad L, Subler MA, Windle JJ, Sarkar D, et al. Knockout of mda-9/syntenin (sdcbp) expression in the microenvironment dampens tumor-supporting inflammation and inhibits melanoma metastasis. *Oncotarget* 2016;7(30):46848-46861.
44. Talukdar S, Das SK, Pradhan AK, Emdad L, Shen XN, Windle JJ, Sarkar D, Fisher PB. Novel function of mda-9/syntenin (sdcbp) as a regulator of survival and stemness in glioma stem cells. *Oncotarget* 2016;7(34):54102-54119.
45. Hwangbo C, Tae N, Lee S, Kim O, Park OK, Kim J, Kwon SH, Lee JH. Syntenin regulates tgf-beta1-induced smad activation and the epithelial-to-mesenchymal transition by inhibiting caveolin-mediated tgf-beta type i receptor internalization. *Oncogene* 2016;35(3):389-401.

46. Wang LK, Pan SH, Chang YL, Hung PF, Kao SH, Wang WL, Lin CW, Yang SC, Liang CH, Wu CT, et al. Mda-9/syntenin-slug transcriptional complex promote epithelial-mesenchymal transition and invasion/metastasis in lung adenocarcinoma. *Oncotarget* 2016;7(1):386-401.
47. Xia Y, Shen S, Verma IM. Nf-kappab, an active player in human cancers. *Cancer immunology research* 2014;2(9):823-830.

Figure Legends

Figure 1: **Syndecan-2 is overexpressed in human lung adenocarcinoma. (*A*)** Syndecan-2 (Sdc2) expression in lung adenocarcinoma tumor core and tumor-free margins was assessed by immunohistochemistry. Sdc2 expression was detected in tumor-affected epithelium (upper right panel) and tissue-associated macrophages in tumor-free margins (upper left panel). Representative images are shown. . **(*B*)** SDC2 mRNA levels were elevated in tumor core samples compared to tumor-free margin samples (n=16; *P<0.05). **(*C*)** Anti-human syndecan-2 antibody was applied to a Lung Cancer Tissue MicroArray (LTMA) in control lung tissue (n=8) and lung adenocarcinoma (n=24). Staining intensity was scored from 1 to 4 (lowest to highest, respectively), showing increased staining in adenocarcinoma tissue compared to controls (*P<0.05). Representative images are shown. **(*D*)** SDC1 and SDC2 mRNA levels were measured in human lungs with adenocarcinoma and control lungs without cancer (n=9). Data represent fold increase of SDC2 expression relative to normal lung tissue. SDC2 levels, but not SDC1 levels, were increased 5 to 35-fold compared to controls (*P<0.05).

Figure 2: **Syndecan-2 potentiates mmp9 expression and enzymatic activity and enhances cell invasion in A549 lung adenocarcinoma cells.** A549 cells were transfected with lentiviral particles carrying either scrambled (scr) or *SDC2* shRNAs. ***(A)*** Transfected cells were transferred onto Matrigel-coated inserts and incubated for 24h to detect invasion. The invaded cells were stained with H&E. Cells transfected with shSDC2 had significantly less invasion compared to Scr-transfected controls. ShSDC2-transfected cells had significantly lower MMP9 ***(B)*** gene expression as determined by RT-PCR and ***(C)*** protein levels and enzymatic activity as determined via Western blot and zymography. The data are

AJRCMB Articles in Press. Published on 18-December-2018 as 10.1165/rcmb.2018-0118OC

presented as mean ± SEM, n=3/group, with testing by Student unpaired t-test (P<0.05; significant comparisons: * vs Scr).

Figure 3: **Overexpression of syndecan-2 enhances mmp9 expression and A549 cell invasion.** Cells were lentivirally transfected with empty vector or pLenti-SDC2-GFP (SDC2-GFP). ***(A)*** Transfection efficiency was confirmed by flow cytometry to detect GFP-positive cells. ***(B)*** and ***(C)*** Transfected cells were lysed and mmp9 expression and cell invasion were determined by Western blot or a Matrigel invasion assay, respectively. The data are presented as mean ± SEM, n=3/group, with testing by Student unpaired t-test (P<0.05; significant comparisons: * vs EV).

Figure 4: **Silencing of MMP9 inhibits A549 cell invasion whereas overexpression reverses shSDC2-mediated inhibition of cell invasion in A549 cells.** ***(A)*** A549 cells were transfected with lentiviral particles carrying either Scr, MMP9 (a) or MMP9 (b) or transiently transfected with pCMV6 (empty vector) or pCMV6-MMP9. Cells were lysed and MMP9 expression was measured via Western blot. ***(B)*** The invasive capacity of Scr and shMMP9 (b)-transfected cells were measured using a Matrigel invasion assay. ***(C)*** Overexpression of MMP9 restored the invasive capacity of cells transfected with shSDC2. The data are presented as mean ± SEM, n=3/group, with testing by Student unpaired t-test or by one-way ANOVA (P<0.05; significant comparisons: * vs EV, † vs shSDC2).

Figure 5: **Syntenin-1 overexpression attenuates shSDC2-mediated effects in A549 cells.** ***(A)*** Scr and shSDC2-transfected cells were lysed and subjected to protein immunoprecipitation by anti-Sdc2 antibody and immunoblotted against syntenin-1 (synt-1). ***(B)*** Cells were lentivirally transfected with pLenti-Syntenin-1-C-Myc-DDK (Synt-1-DDK) or pLenti-C-Myc-DDK (EV). Western blotting was used to measure syntenin-1 expression in cell lysates. ***(C)*** MMP9 expression was measured in cells were transfected with shSDC2 with or without Synt-DDK. Co-transfection with Synt-1-DDK restored expression of MMP9 in cells

transfected with shSDC2. ***(D)*** Co-transfection with Synt-1-DDK almost completely restored the invasive capacity of cells transfected with shSDC2. The data are presented as mean ± SEM, n=3/group, with testing by Student unpaired t-test or by one-way ANOVA (P<0.05; significant comparisons: * vs EV, P<0.05; significant comparisons: † vs shSDC2).

Figure 6: **Silencing of syndecan-2 inhibits nuclear accumulation of NF-κB subunit p65 and its binding to the MMP9 promoter in A549 cells.** Cells were lentivirally transfected with shSDC2 with or without Synt-1-DDK. ***(A)*** Cell lysates underwent nuclear/cytosol fractionation to measure p65 localization. ***(B)*** A chromatin immunoprecipitation (ChIP) assay was used to measure p65 binding to the MMP9 promoter. ***(C)*** and ***(D)*** Cells were transiently transfected with scr or sip65 RNAs for 24 hours prior to being collected to measure MMP9 expression or for the Matrigel invasion assay. The data are presented as mean ± SEM, n=3/group, with testing by Student unpaired t-test (P<0.05; significant comparisons: * vs EV or Scr).

Figure 7: **Silencing of SDC2 attenuates A549 cell tumor growth and micro-metastasis in a xenograft tumor model.** 12 mice were randomly assigned to two groups and subcutaneously injected with 3 x 10^6 Scr A549 cells or shSDC2 A549 cells (n=6 per group). **(*A*)** Tumor volume was measured every 2-3 days for 30 days. The mean tumor volume ± SEM is shown. P<0.05, * vs shSDC2 **(*B*)** Tumors were excised and weighed at day 30 after cell injection. Representative specimens are shown. **(*C*)** Micro-metastasis of A549 cells to the lung was assessed by measuring human DNA in mouse lungs using RT-PCR as described in Methods. The data are presented as mean ± SEM, n=6/group, with testing by Student unpaired t-test (P<0.05; significant comparisons: * vs shSDC2).

AJRCMB Articles in Press. Published on 18-December-2018 as 10.1165/rcmb.2018-0118OC

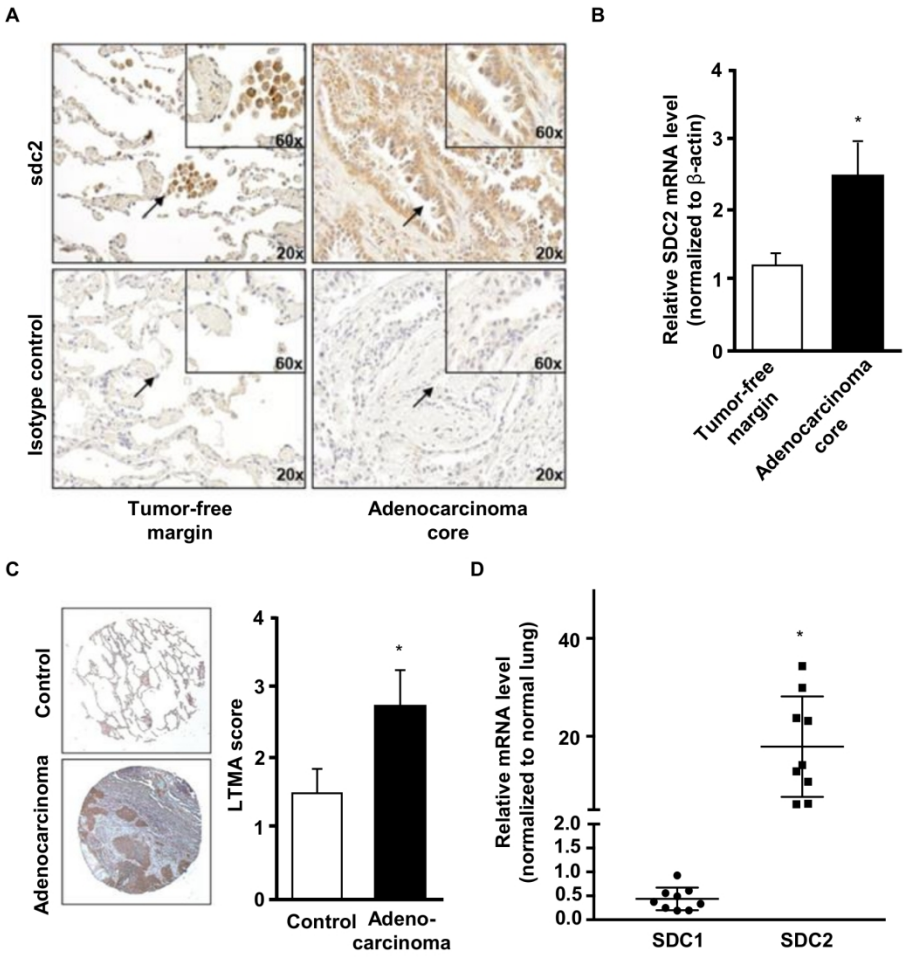

Figure 1

Figure 1: Syndecan-2 is overexpressed in human lung adenocarcinoma. (A) Syndecan-2 (Sdc2) expression in lung adenocarcinoma tumor core and tumor-free margins was assessed by immunohistochemistry. Sdc2 expression was detected in tumor-affected epithelium (upper right panel) and tissue-associated macrophages in tumor-free margins (upper left panel). Representative images are shown. . (B) SDC2 mRNA levels were elevated in tumor core samples compared to tumor-free margin samples (n=16; *P<0.05). (C) Anti-human syndecan-2 antibody was applied to a Lung Cancer Tissue MicroArray (LTMA) in control lung tissue (n=8) and lung adenocarcinoma (n=24). Staining intensity was scored from 1 to 4 (lowest to highest, respectively), showing increased staining in adenocarcinoma tissue compared to controls (*P<0.05). Representative images are shown. (D) SDC1 and SDC2 mRNA levels were measured in human lungs with adenocarcinoma and control lungs without cancer (n=9). Data represent fold increase of SDC2 expression relative to normal lung tissue. SDC2 levels, but not SDC1 levels, were increased 5 to 35-fold compared to controls (*P<0.05).

174x212mm (300 x 300 DPI)

AJRCMB Articles in Press. Published on 18-December-2018 as 10.1165/rcmb.2018-0118OC

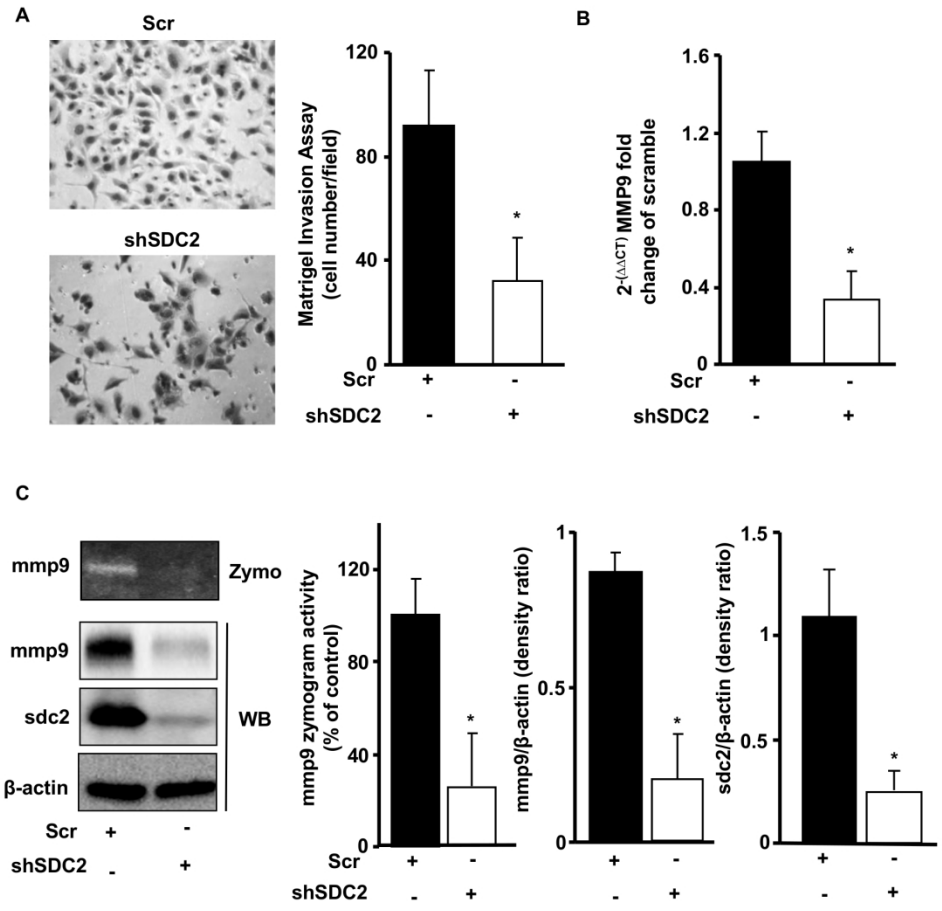

Figure 2

Figure 2: Syndecan-2 potentiates mmp9 expression and enzymatic activity and enhances cell invasion in A549 lung adenocarcinoma cells. A549 cells were transfected with lentiviral particles carrying either scrambled (scr) or SDC2 shRNAs. (A) Transfected cells were transferred onto Matrigel-coated inserts and incubated for 24h to detect invasion. The invaded cells were stained with H&E. Cells transfected with shSDC2 had significantly less invasion compared to Scr-transfected controls. ShSDC2-transfected cells had significantly lower MMP9 (B) gene expression as determined by RT-PCR and (C) protein levels and enzymatic activity as determined via Western blot and zymography. The data are presented as mean ± SEM, n=3/group, with testing by Student unpaired t-test ($P<0.05$; significant comparisons: * vs Scr).

174x212mm (300 x 300 DPI)

AJRCMB Articles in Press. Published on 18-December-2018 as 10.1165/rcmb.2018-0118OC

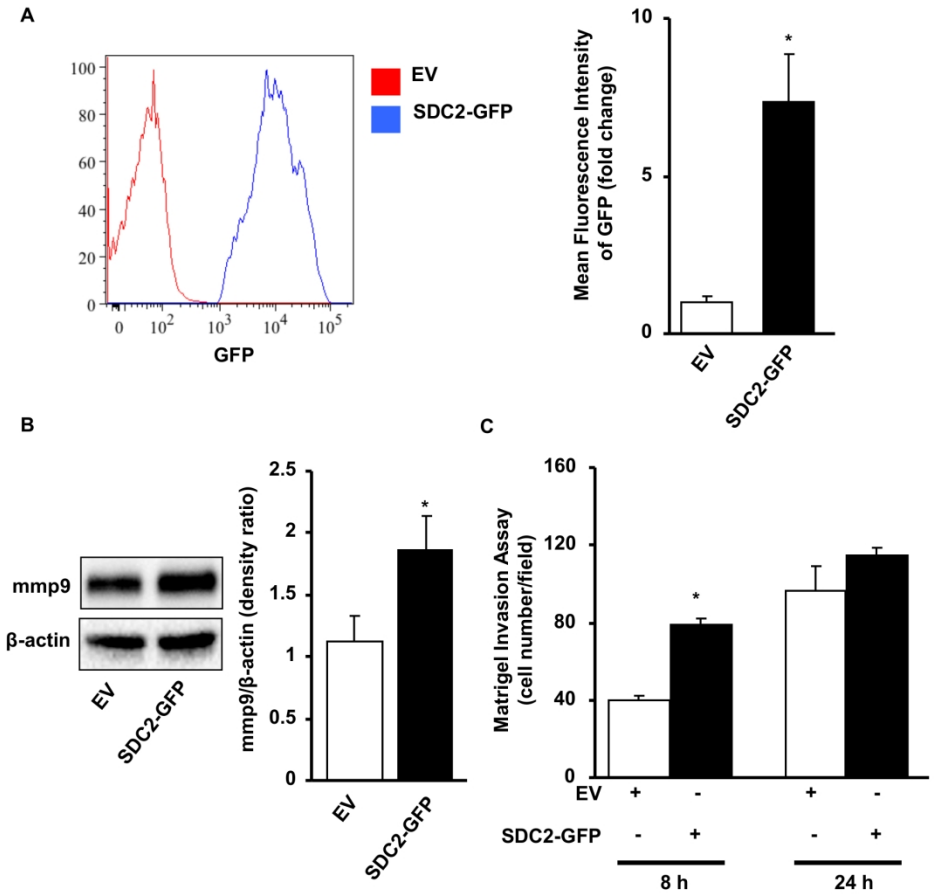

Figure 3

Figure 3: Overexpression of syndecan-2 enhances mmp9 expression and A549 cell invasion. Cells were lentivirally transfected with empty vector or pLenti-SDC2-GFP (SDC2-GFP). (A) Transfection efficiency was confirmed by flow cytometry to detect GFP-positive cells. (B) and (C) Transfected cells were lysed and mmp9 expression and cell invasion were determined by Western blot or a Matrigel invasion assay, respectively. The data are presented as mean ± SEM, n=3/group, with testing by Student unpaired t-test ($P<0.05$; significant comparisons: * vs EV).

174x212mm (300 x 300 DPI)

AJRCMB Articles in Press. Published on 18-December-2018 as 10.1165/rcmb.2018-0118OC

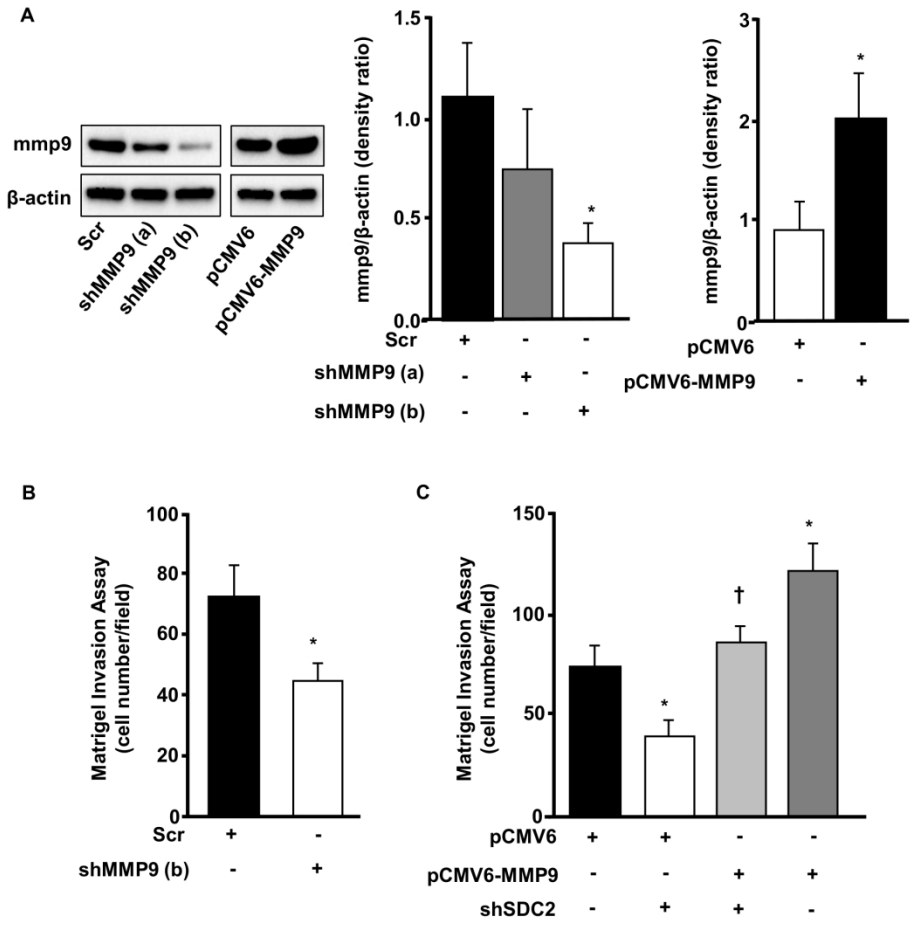

Figure 4

Figure 4: Silencing of MMP9 inhibits A549 cell invasion whereas overexpression reverses shSDC2-mediated inhibition of cell invasion in A549 cells. (A) A549 cells were transfected with lentiviral particles carrying either Scr, MMP9 (a) or MMP9 (b) or transiently transfected with pCMV6 (empty vector) or pCMV6-MMP9. Cells were lysed and MMP9 expression was measured via Western blot. (B) The invasive capacity of Scr and shMMP9 (b)-transfected cells were measured using a Matrigel invasion assay. (C) Overexpression of MMP9 restored the invasive capacity of cells transfected with shSDC2. The data are presented as mean ± SEM, n=3/group, with testing by Student unpaired t-test or by one-way ANOVA (P<0.05; significant comparisons: * vs EV, † vs shSDC2).

174x212mm (300 x 300 DPI)

AJRCMB Articles in Press. Published on 18-December-2018 as 10.1165/rcmb.2018-0118OC

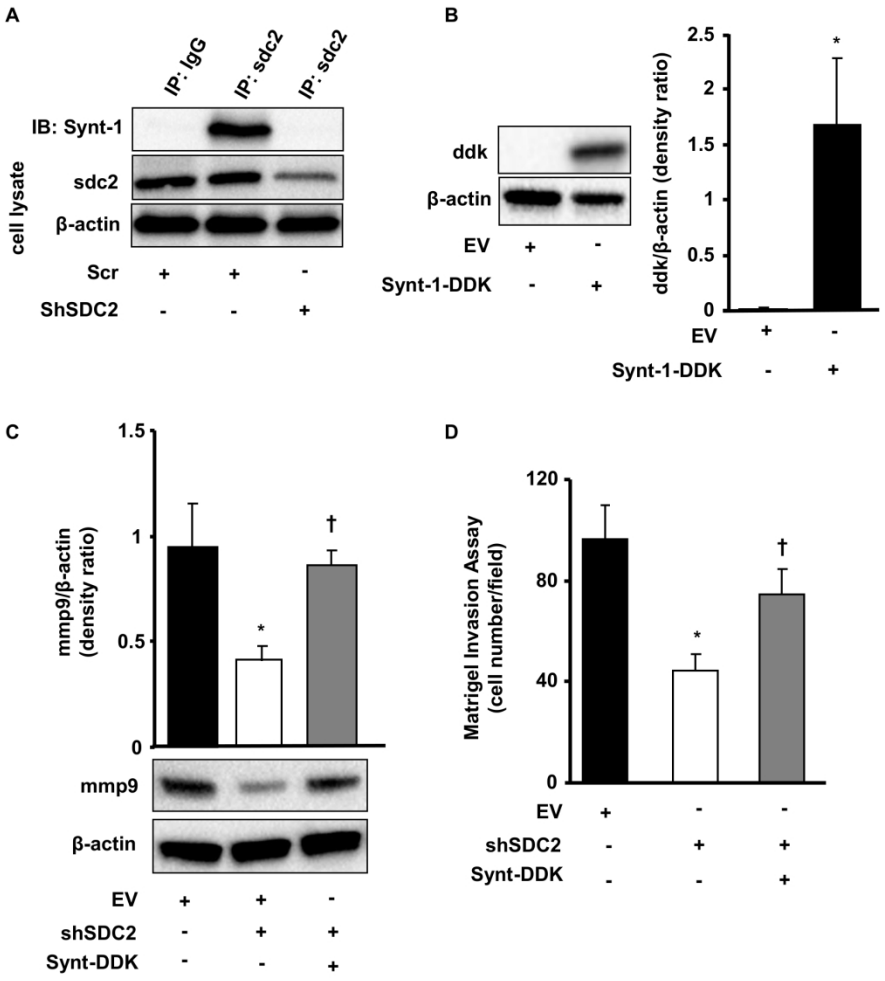

Figure 5

Figure 5: Syntenin-1 overexpression attenuates shSDC2-mediated effects in A549 cells. (A) Scr and shSDC2-transfected cells were lysed and subjected to protein immunoprecipitation by anti-Sdc2 antibody and immunoblotted against syntenin-1 (synt-1). (B) Cells were lentivirally transfected with pLenti-Syntenin-1-C-Myc-DDK (Synt-1-DDK) or pLenti-C-Myc-DDK (EV). Western blotting was used to measure syntenin-1 expression in cell lysates. (C) MMP9 expression was measured in cells were transfected with shSDC2 with or without Synt-DDK. Co-transfection with Synt-1-DDK restored expression of MMP9 in cells transfected with shSDC2. (D) Co-transfection with Synt-1-DDK almost completely restored the invasive capacity of cells transfected with shSDC2. The data are presented as mean ± SEM, n=3/group, with testing by Student unpaired t-test or by one-way ANOVA ($P<0.05$; significant comparisons: * vs EV, $P<0.05$; significant comparisons: † vs shSDC2).

174x212mm (300 x 300 DPI)

AJRCMB Articles in Press. Published on 18-December-2018 as 10.1165/rcmb.2018-0118OC

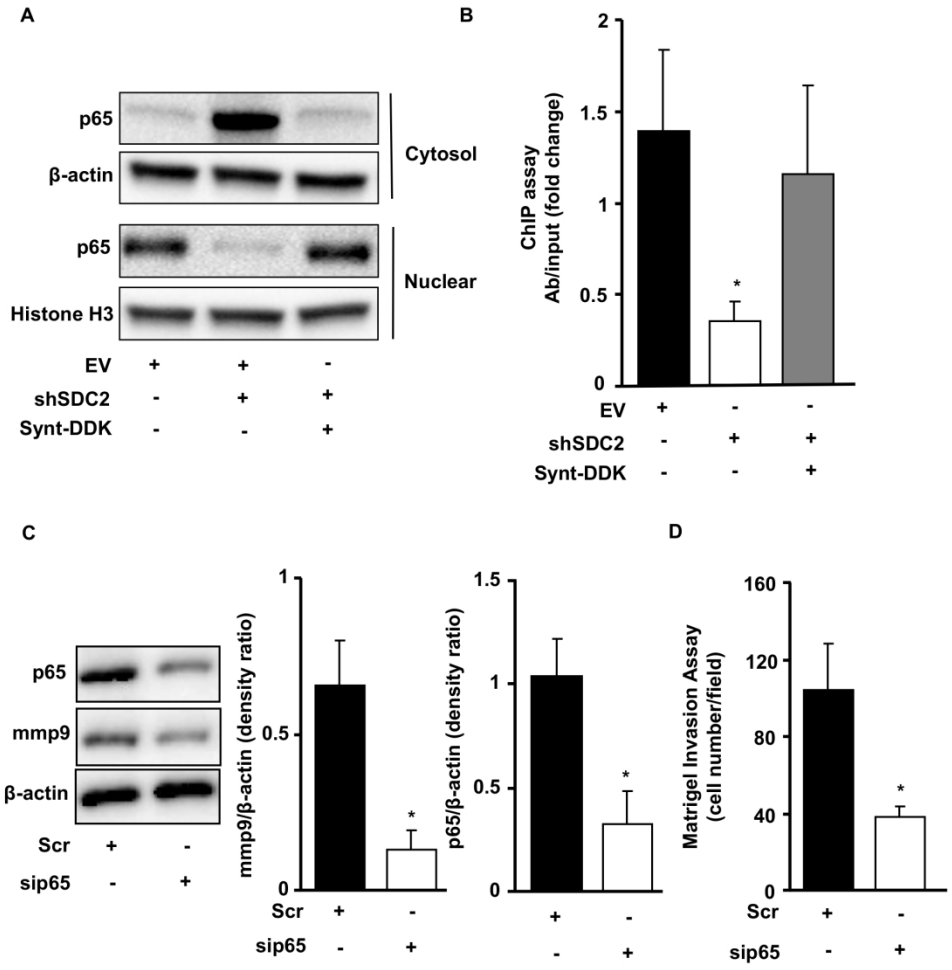

Figure 6

Figure 6: Silencing of syndecan-2 inhibits nuclear accumulation of NF-κB subunit p65 and its binding to the MMP9 promoter in A549 cells. Cells were lentivirally transfected with shSDC2 with or without Synt-1-DDK. (A) Cell lysates underwent nuclear/cytosol fractionation to measure p65 localization. (B) A chromatin immunoprecipitation (ChIP) assay was used to measure p65 binding to the MMP9 promoter. (C) and (D) Cells were transiently transfected with scr or sip65 RNAs for 24 hours prior to being collected to measure MMP9 expression or for the Matrigel invasion assay. The data are presented as mean ± SEM, n=3/group, with testing by Student unpaired t-test ($P<0.05$; significant comparisons: * vs EV or Scr).

174x212mm (300 x 300 DPI)

AJRCMB Articles in Press. Published on 18-December-2018 as 10.1165/rcmb.2018-0118OC

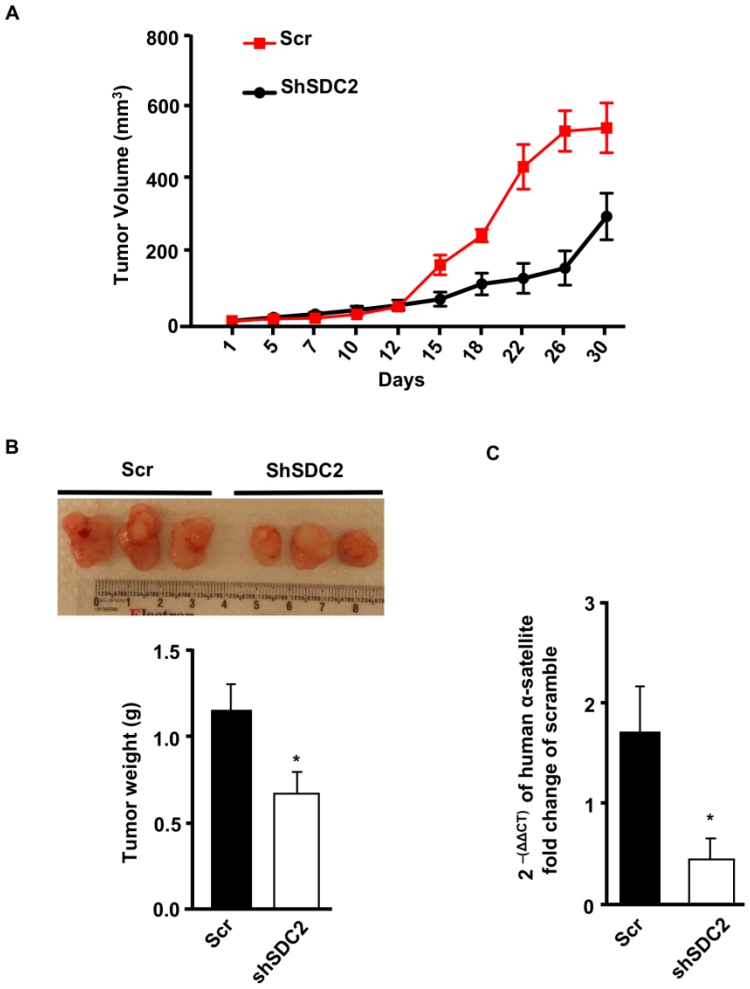

Figure 7

Figure 7: Silencing of SDC2 attenuates A549 cell tumor growth and micro-metastasis in a xenograft tumor model. 12 mice were randomly assigned to two groups and subcutaneously injected with 3 x 106 Scr A549 cells or shSDC2 A549 cells (n=6 per group). (A) Tumor volume was measured every 2-3 days for 30 days. The mean tumor volume ± SEM is shown. P<0.05, * vs shSDC2 (B) Tumors were excised and weighed at day 30 after cell injection. Representative specimens are shown. (C) Micro-metastasis of A549 cells to the lung was assessed by measuring human DNA in mouse lungs using RT-PCR as described in Methods. The data are presented as mean ± SEM, n=6/group, with testing by Student unpaired t-test (P<0.05; significant comparisons: * vs shSDC2).

174x212mm (300 x 300 DPI)

AJRCMB Articles in Press. Published on 18-December-2018 as 10.1165/rcmb.2018-0118OC

ONLINE DATA SUPPLEMENT

Lung Adenocarcinoma Syndecan-2 Potentiates Cell Invasiveness

Konstantin Tsoyi[1#], Juan C Osorio[1,2#], Sarah G Chu[1], Isis E Fernandez[3], Sergio Poli[1], Lynette Sholl[4], Ye Cui[1], Carmen S Tellez[5], Jill M Siegfried[6], Steven A Belinsky[5], Mark A. Perrella[1], Souheil El-Chemaly[1], Ivan O. Rosas[1,7]

[1]Division of Pulmonary and Critical Care Medicine, Brigham and Women's Hospital, Harvard Medical School, Boston, MA, [2]Department of Medicine, New York Presbyterian Hospital, Weill Cornell Medical College, New York, NY, [3]Comprehensive Pneumology Centre, Hospital of the Ludwig-Maximilians, University of Munich, Munich, [4]Department of Pathology, Brigham and Women's Hospital, Harvard Medical School, Boston, MA, [5]Lung Cancer Program, Lovelace Respiratory Research Institute, Albuquerque, NM, [6]University of Minnesota, Department of Pharmacology, Minneapolis, Minnesota, United States, [7]Pulmonary Fibrosis Group, Lovelace Respiratory Research Institute, Albuquerque NM

[#] Authors contributed equally to this work

Running title: Syndecan-2 is elevated in lung adenocarcinoma

Corresponding Author:

Ivan O. Rosas, M.D.

Division of Pulmonary and Critical Care Medicine

Brigham and Women's Hospital

75 Francis Street, Boston, MA 02115

E-mail: irosas@rics.bwh.harvard.edu

AJRCMB Articles in Press. Published on 18-December-2018 as 10.1165/rcmb.2018-0118OC

Supplemental Materials and Methods:

Gelatin Zymography

MMP9 activity in A549 culture medium was determined using gelatin zymography as described previously (1). Cells were plated in equal numbers onto 6-well plates. After treatment, the conditioned medium was collected and concentrated 20-fold using Centricon filters (Millipore, Bedford, MA). Equal amounts of concentrated medium were mixed with 2x buffer and resolved using 8% SDS-PAGE gels containing 1 mg/mL gelatin. After electrophoresis, gels were washed twice with 2.5% Triton X-100 for 30 min at room temperature and incubated with developing buffer (50 mM Tris–Cl, pH 7.6, 5 mM CaCl2, 0.02% Brij-35) overnight at 37 °C. Gels were subsequently stained with 0.2% Coomassie Brilliant Blue R-250 in 50% methanol and 10% glacial acetic acid, and then destained in the same solution without the dye. MMP9 activity was visualized as clear bands within the stained gel.

Lentiviral Transfection

PLKO.1 plasmids carrying either the human shSDC2 target sequence CCGGCCAGCCGAAGAGGATAC (consortium number TRCN0000286560), shMMP9 (a) target sequence CCACAACATCACCTATTGGAT (consortium number TRCN0000051438), shMMP9 (b) target sequence CATTCAGGGAGACGCCCATTT (consortium number TRCN0000373008) or a scrambled (Scr) sequence were purchased from Sigma-Aldrich (St. Louis, MO). Lentiviral particles were generated by use of a commercially available packaging mix (Cat. #: SHP001; Sigma-Aldrich, St Louis, MO) in human embryonic kidney 293 T cells according to the manufacturer's instructions. A549 cells were infected with the lentiviral particles, and stably selected by use of puromycin (10 μg/mL). To overexpress human syntenin-1 and syndecan-2, pLenti-C-Myc-DDK plasmids carrying the syntenin-1 open reading frame and pLenti-C-mGFP plasmids carrying the syndecan-2 open reading frame were purchased from Origene (Rockville,

AJRCMB Articles in Press. Published on 18-December-2018 as 10.1165/rcmb.2018-0118OC

MD). Lentiviral particles were generated by use of a commercially available packaging mix (Cat. #: TR30037; Origene, Rockville, MD) in human embryonic kidney 293 T cells, according to the manufacturer's instructions.

Transient Transfection

SiScr and sip65 were provided by Cell Signaling Technology (Beverly, MA); pCMV6 and pCMV6-MMP9 were purchased from Origene, Rockville, MD. Transient transfection was performed using Superfect from Qiagen (Valencia, CA) according to the manufacturer's protocol. Briefly, 1 x 10^5 cells were plated onto 60-mm dishes (or 1 x 10^7 cells onto 100 mm dishes) the day before transfection and grown to approximately 70% confluence. The transfections were allowed to proceed for 8 h. Transfected cells were washed with 4 mL of PBS and used for further experiments.

Real Time-PCR

Total RNA was isolated using the RNeasy Mini Kit from Qiagen (Valencia, CA) and reverse transcribed. SDC2, MMP9 and GAPDH expression were analyzed by quantitative real-time PCR using SYBR Green qPCR Master Mix (GenDEPOT, Barker, TX), and specific primers for human syndecan-2 (sense: 5'CAACATCTCGACCACTTCCA3'; anti-sense: 5'TGGGTCCATTTTCCTTTCTG3'), MMP-9 (sense: ACGACGTCTTCCAGTACCGA; anti-sense: TTGGTCCACCTGGTTCAACT), GAPDH (sense: CGCTGAGTACGTCGTGG AGTC; anti-sense: GCTGATGATCTTGAGGCTGTTGTC). Signal generation was normalized to GAPDH. Fold changes for transcripts were normalized to control samples using the ΔΔCT formula.

Western Immunoblotting

Western blot experiments were performed as previously described (2-4). Cells were lysed using radio-immunoprecipitation assay (RIPA) buffer containing sodium ortho-vanadate (Sigma, St

AJRCMB Articles in Press. Published on 18-December-2018 as 10.1165/rcmb.2018-0118OC

Louis, MO) and a cocktail of protease inhibitors (Roche Applied Science, Indianapolis, IN). In select experiments, fractionation of nuclear and cytoplasmic proteins was performed using the Qproteome cell compartment kit (Qiagen, Valencia, CA). Cells were harvested and lysed according to the manufacturer's protocol. The fractionated proteins were concentrated and desalted by acetone precipitation for Western blot analysis. Protein concentration was determined using the BCA protein assay kit (Pierce, Rockford, IL). Proteins were separated by SDS-PAGE and transferred to a Polyscreen PVDF membrane (Perkin Elmer Life Sciences, Waltham, MA). Membranes were blocked with 5% non-fat dry milk in Tris-buffered saline + 0.05% Tween®20 (TBS-T) and incubated overnight at 4 °C with primary antibody dilutions in TBS-T. After washing in TBS-T, the membranes were incubated in cognate horseradish peroxidase (HRP)-conjugated secondary antibody for an hour at room temperature, washed again with TBS-T, and proteins were detected by chemiluminescence (Amersham Biosciences, Pittsburgh, PA). The β-actin antibody was used as a standard for protein loading.

Co-immunoprecipitation

For co-immunoprecipitation (Co-IP) of syntenin-1 with syndecan-2, Scramble and shSDC2-transfected A549 cells were plated onto 100 mm dishes. Cells were lysed using RIPA buffer, lysates were clarified by centrifuging at 15,000 g for 15 min, and pre-cleared by incubating with protein A-Sepharose (Santa Cruz, CA) for 2 hours at 4 °C. Supernatants were transferred to separate 1.5 mL microcentrifuge tubes containing syndecan-2 primary antibody or appropriate controls (beads alone, normal IgG) prebound to protein-A Sepharose. After incubation by rotating overnight at 4 °C, immunoprecipitates were washed 5 times with RIPA buffer and subjected to immunoblot analysis with the anti-syntenin-1 antibody.

Matrigel Invasion Assay

AJRCMB Articles in Press. Published on 18-December-2018 as 10.1165/rcmb.2018-0118OC

Invasion assays with A549 or NCI-H23 cells were performed as previously described (1). Briefly, cells were cultured for 3 days. The upper chamber of 24-well cell culture inserts (8 μm pore size, Falcon, Franklin Lakes, NJ) were washed with a serum-free medium, coated with 100 μL of Matrigel (1 mg/mL) and dried for 30 min at 37 °C. 2 x 10^5 cells per insert were seeded to the upper chambers and 500 μL of DMEM containing 10% FBS were added to the lower chambers. The invasion chambers were incubated for 24 h in a 37 °C cell culture incubator. Non-invasive cells that remained on the upper surface of the insert membranes were removed by scrubbing. Cells on the lower insert membrane were stained with 0.6% hematoxylin and 0.5% eosin and were counted under light microscopy. Each sample was assayed in triplicate and each experiment was repeated 3 times.

Chromatin Immunoprecipitation (ChIP) Assay

The ChIP assay was performed by use of an enzymatic Chromatin IP kit from Cell Signaling Technology (Cat. #: 9002, Danvers, CA) according to the manufacturer's instructions. In brief, A549 cells were fixed in 1% formaldehyde for 10 min at room temperature. Cross-linking was stopped by adding glycine. DNA was digested by use of micrococcal nuclease to the length of ~150-900 bp. Before incubation with antibodies, 10 μL of input control solution was taken from each sample. The remaining chromatin solution was incubated with 10 μg anti-p65 antibody at 4 °C overnight (Cell Signaling Technology). Immune complexes were precipitated, washed, and eluted as recommended. DNA-protein cross-links were reversed by heating at 65 °C for 2 h, and 10 μL of each sample was used as a template for qRT-PCR. MMP-9 oligonucleotide sequences for PCR primers were forward 5′- ATTCAGCCTGCGGAAGACCAG-3′ and reverse 5′-ACTCCAGGCTCTGTCCTCTT-3′. This primer set encompasses the MMP9 promoter segment from -634 to -484. The relative quantity of target MMP9 promoter was calculated by use of the CT method (Sequence Detection System software, version 1.7; Applied Biosystems), or $2^{-\Delta\Delta CT}$,

AJRCMB Articles in Press. Published on 18-December-2018 as 10.1165/rcmb.2018-0118OC

as described (5). The $2^{-\Delta\Delta CT}$ from immunoprecipitation samples by use of p65 antibodies was normalized with the $2^{-\Delta\Delta CT}$ from the input control samples and graphed as a percentage of the control samples.

Xenograft tumor model

Severe combined immunodeficient (SCID) female mice (n=12, 8-10 weeks old) were purchased from Jackson Laboratory. 3 x 10^6 A549 cells were suspended in Matrigel and injected subcutaneously. Tumor growth was measured 2-3 times a week. Tumor volume was estimated as the product of the longest diameter and the square of its perpendicular (i.e, width) divided by two. Thirty days after cell injection, tumors and lungs were harvested. To verify the presence of human cells in mouse lungs, RT-PCR was used to detect the alpha-satellite DNA sequence of the centromere region of human chromosome 17, as previously described by Becker et al. (6).

Supplemental Figure Legends:

Figure E1: **Syndecan-2 is increased in different types of lung carcinoma.** Anti-human syndecan-2 (sdc2) antibody was applied to a Lung Cancer Tissue MicroArray (LTMA) with normal lung tissue (n=8), squamous cell carcinoma (n=24), adenocarcinoma (n=24), adenoaquamous carcinoma (n=6), small cell carcinoma (n=6) and papillary adenocarcinoma (n=8). Staining intensity was scored from 1 to 4 (lowest to highest, respectively). Sdc2 staining intensity was increased in carcinoma tissue compared to control (*P<0.05).

Figure E2: **Syndecan-2, NF-κB (p65) and mmp9 staining are increased in lung adenocarcinoma and A549 cells.** Normal lung (n=3), lung adenocarcinoma (n=5) tissue slides and A549 cells (n=3) were incubated with sdc2, p65 and mmp9 antibodies and then

AJRCMB Articles in Press. Published on 18-December-2018 as 10.1165/rcmb.2018-0118OC

counterstained with hematoxylin. Representative images are shown. The scale bar represents 100 μm.

Figure E3: **Syndecan-2 regulates mmp9 expression and cell invasion in NCI-H23 cells.** NCI-H23 cells were transfected with Scr, shSDC2 or shMMP9 lentiviral particles. Transfected cells were transferred onto Matrigel-coated inserts, which were incubated for 24 h. Invaded cells were then stained and counted. Cells transfected with shSDC2 and shMMP9 had significantly decreased invasion compared to Scr-transfected controls. The data are presented as mean ± SEM, n=3/group, with testing by Student unpaired t-test ($P<0.05$; significant comparisons: * vs Scr).

References:

1. Kim YM, Tsoyi K, Jang HJ, Park EJ, Park SW, Kim HJ, Hwa JS, Chang KC. CKD712, a synthetic isoquinoline alkaloid, enhances the anti-cancer effects of paclitaxel in MDA-MB-231 cells through regulation of PTEN. *Life sciences* 2014; 112: 49-58.
2. Tsoyi K, Geldart AM, Christou H, Liu X, Chung SW, Perrella MA. Elk-3 is a KLF4-regulated gene that modulates the phagocytosis of bacteria by macrophages. *Journal of leukocyte biology* 2015; 97: 171-180.
3. Tsoyi K, Jang HJ, Nizamutdinova IT, Kim YM, Lee YS, Kim HJ, Seo HG, Lee JH, Chang KC. Metformin inhibits HMGB1 release in LPS-treated RAW 264.7 cells and increases survival rate of endotoxaemic mice. *British journal of pharmacology* 2011; 162: 1498-1508.
4. Tsoyi K, Kim HJ, Shin JS, Kim DH, Cho HJ, Lee SS, Ahn SK, Yun-Choi HS, Lee JH, Seo HG, Chang KC. HO-1 and JAK-2/STAT-1 signals are involved in preferential inhibition of iNOS over COX-2 gene expression by newly synthesized tetrahydroisoquinoline alkaloid, CKD712, in cells activated with lipopolysacchride. *Cellular signalling* 2008; 20: 1839-1847.
5. Schmittgen TD, Livak KJ. Analyzing real-time PCR data by the comparative C(T) method. *Nature protocols* 2008; 3: 1101-1108.
6. Becker M, Nitsche A, Neumann C, Aumann J, Junghahn I, Fichtner I. Sensitive PCR method for the detection and real-time quantification of human cells in xenotransplantation systems. *British journal of cancer* 2002; 87: 1328-1335.

AJRCMB Articles in Press. Published on 18-December-2018 as 10.1165/rcmb.2018-0118OC

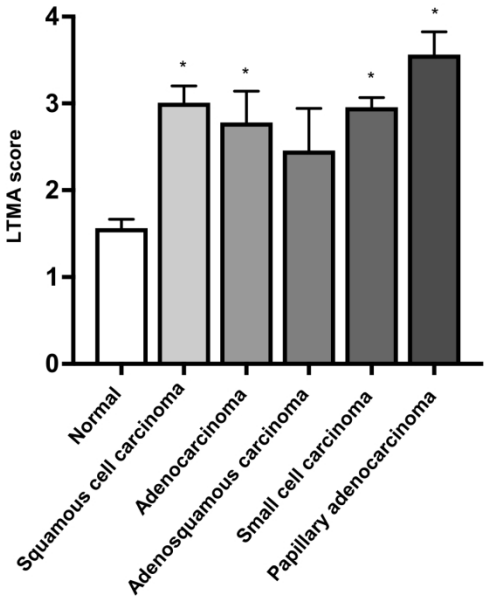

Figure E1

Figure E1: Syndecan-2 is increased in different types of lung carcinoma. Anti-human syndecan-2 (sdc2) antibody was applied to a Lung Cancer Tissue MicroArray (LTMA) with normal lung tissue (n=8), squamous cell carcinoma (n=24), adenocarcinoma (n=24), adenoaquamous carcinoma (n=6), small cell carcinoma (n=6) and papillary adenocarcinoma (n=8). Staining intensity was scored from 1 to 4 (lowest to highest, respectively). Sdc2 staining intensity was increased in carcinoma tissue compared to control (*P<0.05).

174x212mm (300 x 300 DPI)

AJRCMB Articles in Press. Published on 18-December-2018 as 10.1165/rcmb.2018-0118OC

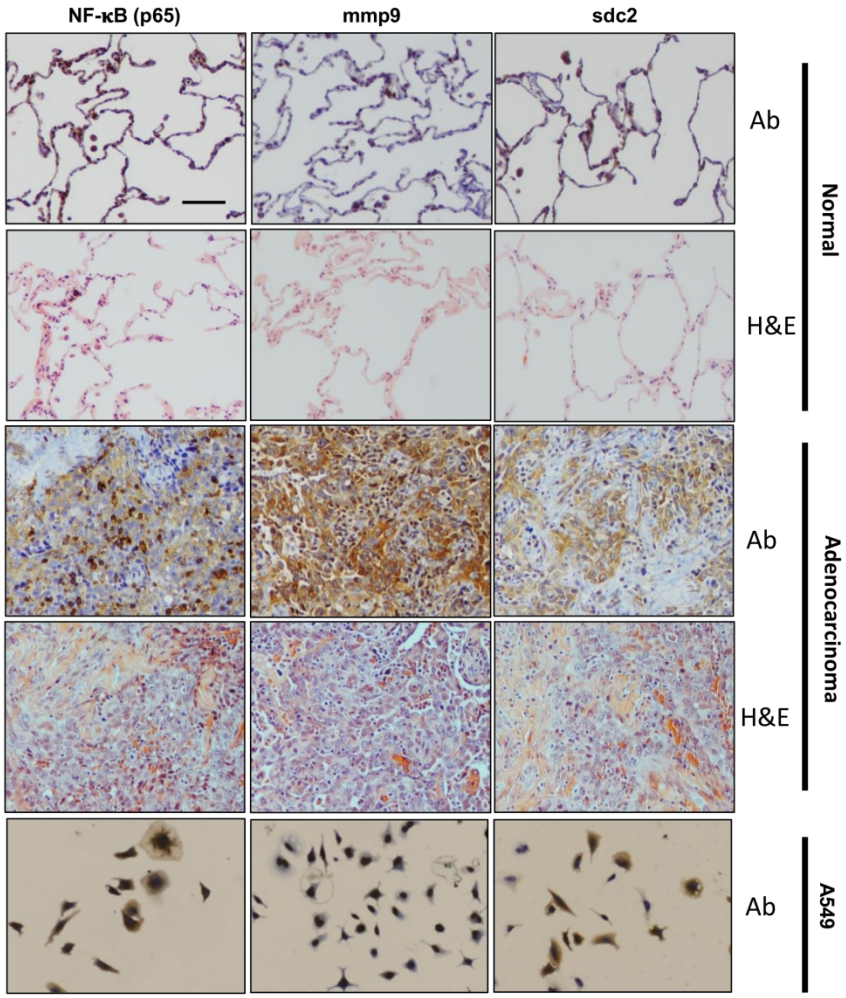

Figure E2

Figure E2: Syndecan-2, NF-□B (p65) and mmp9 staining are increased in lung adenocarcinoma and A549 cells. Normal lung (n=3), lung adenocarcinoma (n=5) tissue slides and A549 cells (n=3) were incubated with sdc2, p65 and mmp9 antibodies and then counterstained with hematoxylin. Representative images are shown. The scale bar represents 100 □m.

174x212mm (300 x 300 DPI)

AJRCMB Articles in Press. Published on 18-December-2018 as 10.1165/rcmb.2018-0118OC

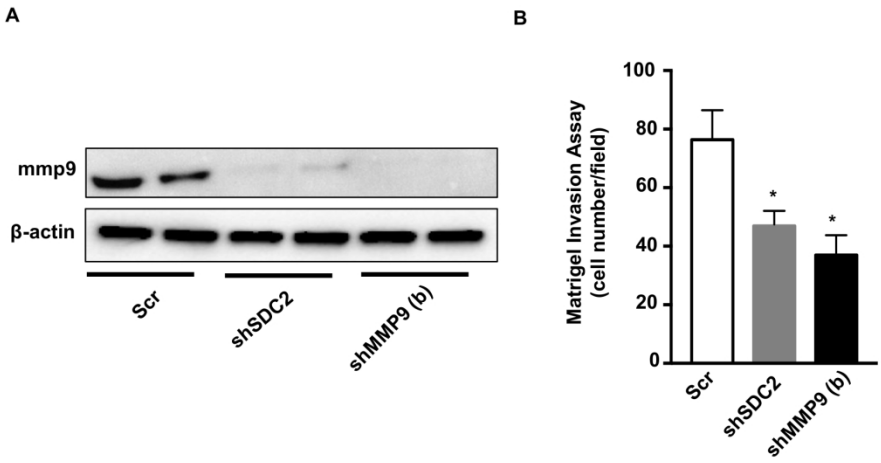

Figure E3

Figure E3: Syndecan-2 regulates mmp9 expression and cell invasion in NCI-H23 cells. NCI-H23 cells were transfected with Scr, shSDC2 or shMMP9 lentiviral particles. Transfected cells were transferred onto Matrigel-coated inserts, which were incubated for 24 h. Invaded cells were then stained and counted. Cells transfected with shSDC2 and shMMP9 had significantly decreased invasion compared to Scr-transfected controls. The data are presented as mean ± SEM, n=3/group, with testing by Student unpaired t-test ($P<0.05$; significant comparisons: * vs Scr).

174x212mm (300 x 300 DPI)